Received: 8 July 2020 | Revised: 3 October 2020 | Accepted: 5 October 2020

DOI: 10.1002/eng2.12315

SHORT COMMUNICATION

WILEY

Mechanically flexible viscosity sensor for real-time monitoring of tubular architectures for industrial applications

Maha A. Nour[1] | **Sherjeel M. Khan**[1] | **Nadeem Qaiser**[1] | **Saleh A. Bunaiyan**[1,2] | **Muhammad M. Hussain**[1,3]

[1]mmh Labs, Electrical and Computer Engineering, Computer Electrical Mathematical Science and Engineering Division, King Abdullah University of Science and Technology (KAUST), Thuwal, Saudi Arabia

[2]EE, College of Engineering, King Fahd University of Petroleum and Minerals (KFUPM), Dhahran, Saudi Arabia

[3]EECS, University of California, Berkeley, Berkeley, California, USA

Correspondence
Muhammad M. Hussain, EECS, University of California, Berkeley, Berkeley, CA 94720.
Email: mmhussain@berkeley.edu

Funding information
King Abdullah University of Science and Technology, Grant/Award Number: BAS/1/1619-01-01; Saudi Aramco

Abstract

Real-time monitoring of fluid viscosities in tubular systems is essential for industries transporting fluid media. The available real-time viscometers for tubular systems have major drawbacks, such as using invasive methods with large pressure drops due to flow disturbances, destructive installation processes with permanent tube damage, and limited operability with laminar flows. Therefore, developing a viscometer to address the above-mentioned concerns is required for industrial applications. In this study, a new application of a velocity-dependent viscometer using a novel design for real-time measurements with insignificant flow disruption is proposed. It involves a Poly (methyl-methacrylate) microchannel bridge with a microfluidic flowmeter attached to a mechanically flexible Polydimethylsiloxane platform connected to the inner surface of the pipe, which can adapt to different pipe diameters and curvatures. Moreover, the proposed viscometer uses the pipe flow driving force to flow fluids into the microchannel for measurement without requiring a pumping system or any sample withdrawals. The results of the simulation analysis match the experimental results of the sensor performance. The sensor can measure different viscosities in the range of 4-334 mPa s with a resolution higher than 2.7 mPa s. Finally, a stand-alone system is integrated with the sensor for wireless data transmission.

KEYWORDS

flexible, microfluidic, pipe, tube, viscometer

1 | INTRODUCTION

Monitoring of fluids' viscosities is essential for industries engaged in transporting fluids in tubular systems such as pipes. It is crucial to plan the pumping systems and select the required initial pressure to transfer fluids from one location to another.[1,2] Moreover, viscosity analysis is employed to ensure product consistency as a quality indicator within the industrial production process, such as in petrochemical,[3-5] polymers,[6-8] and food industries.[9-11] Capillary methods,[12,13] falling-object methods,[14,15] vibrational,[16-18] optical[19-21] and torque detection are various known and reliable techniques for

measuring the viscosity using an off-line workstation setup.[22-24] The conventional approach for the viscosity measurement procedures in industries starts with on-site sample collection, followed by laboratory analysis, and, sometimes, requiring sample preparation before examination; it ends with sending the results' report to the site for decision-making.[25] However, this is a time-consuming and inefficient process for the rapid industrial growth with their increasing demands. Therefore, reliable real-time viscosity sensors for tubular systems are desirable for industries to allow adequate production controls and reduce costs through accurate decisions, decreasing production errors, and lower fluid wastes.

Numerous viscometers have been developed for real-time monitoring in tubular systems.[26] The available viscosity sensors for this purpose are classified into three categories according to their operating principles, vibrational,[27,28] rotational,[29,30] and change in fluid velocity-based measurement sensors.[31-33] The vibrational and rotational viscometers are large and rigid instruments that interfere with the liquids in the tubular systems and disturb the fluid flow creating a pressure drop and subsequent energy loss. In addition, some of them are destructive techniques that require access to the fluid through the pipe, causing a permanent damage to the pipe. The viscometer based on the change in fluid velocity or pressure drop is a simple and inexpensive measurement apparatus based on the Hagen-Poiseuille law.[34,35] It can be based on a non-invasive and non-destructive method by selecting the appropriate flowmeters to measure the change in the velocity profile, such as using probes (for example, ultrasonic and electromagnetic sensors[36-38]) attached to the outer surface of the pipe. However, the main drawback of this technology is that its operation is restricted to the laminar flow condition.[39,40] Hence, there is still a demand for developing reliable in-line viscometers to meet the industrial needs.

On the other hand, real-time viscometers have been robustly established and well developed for microfluidic monitoring applications. Microelectromechanical systems (MEMS),[41-43] micro-resonators,[44,45] and fluid velocity-based measurements are common types of real-time microfluidic viscometers.[46,47] These sensors are particularly optimized for microfluidic applications, where the MEMS and micro-resonators are suitable when low volumes of fluid are used. Optical measurements require transparent materials. The fluid velocity-based viscometers, known as micro-capillary viscometers, are limited to laminar flows, where such conditions are assured in microfluidic applications due to the small cross-sectional area of the microchannels.[48] In micro-capillary viscometers, the fluid velocity is determined using the time recorded for the fluid to pass from point to another in identified channel dimensions with the help of microscopic video recording devices or optical sensors.[49,50] The fluid flow rate is obtained based on the pressure drop approach using either micro-pressure sensors as MEMS or capacitive sensors distributed along the channel.[51-53] Near real-time viscosity results have been provided by such micro-viscometers utilized for industrial on-site analyses supported by a pumping system, such as the commercial handheld product viscosity-rheometer-on-chip, to test manually withdrawn fluid samples.[54]

In this paper, we present a new utilization method of the microfluidic viscometer for real-time monitoring of fluids in tube systems. A fluid velocity-based viscometer supported with capacitive pressure sensors distributed along the microchannel is used here. We demonstrate a novel sensor design to overcome the main discussed challenges regarding the real-time monitoring of fluid viscosities in the tube systems. The design involves constructing a microchannel bridge on a mechanically flexible platform attached to the internal tube wall. The physically flexible platform adopts the inner tube surface to match the variations of the pipes' diameters and the different structures' curvatures as well as to provide low flow disturbance and pressure drop using a small depth value of the device. The proposed viscometer is developed with low-cost materials and fabrication processes to make it affordable. The microchannel bridge uses the fluid flow of the tube to drive a small fluid volume into the microfluidic channel, as a continuous flow, for viscosity measurements without requiring any external pump or withdrawn samples from the system. The flow rate inside the microchannel depends on the pipe fluid viscosity. We focused our study assuming incompressible Newtonian fluids. Results showed that the numerical analysis agreed with the experimental work, and moreover, the fluid viscosity is inversely proportional to the microchannel flow rate that can be translated into a change in the pressure or measured capacitance.

2 | MATERIALS AND STRUCTURAL DESIGN

Figure 1 demonstrates the materials used and structural design of the viscometer, which consists of a microchannel attached to the internal tube wall to monitor the viscosity of the fluid using a microfluidic flow sensor installed in the microchannel. The viscometer design is developed using a Poly (methyl-methacrylate) (PMMA) bridge that is positioned on a physically flexible platform to form the microchannel. PMMA was selected as it is a mechanically solid material that ensures constant channel dimensions by resisting channel deformations even under various applied pressures resulting from the surrounding liquid environment. The design of the microchannel ensures the laminar flow of fluid inside it, regardless of the flow type in the tube system, by providing a small hydraulic diameter (D_h) and decreasing the Reynolds

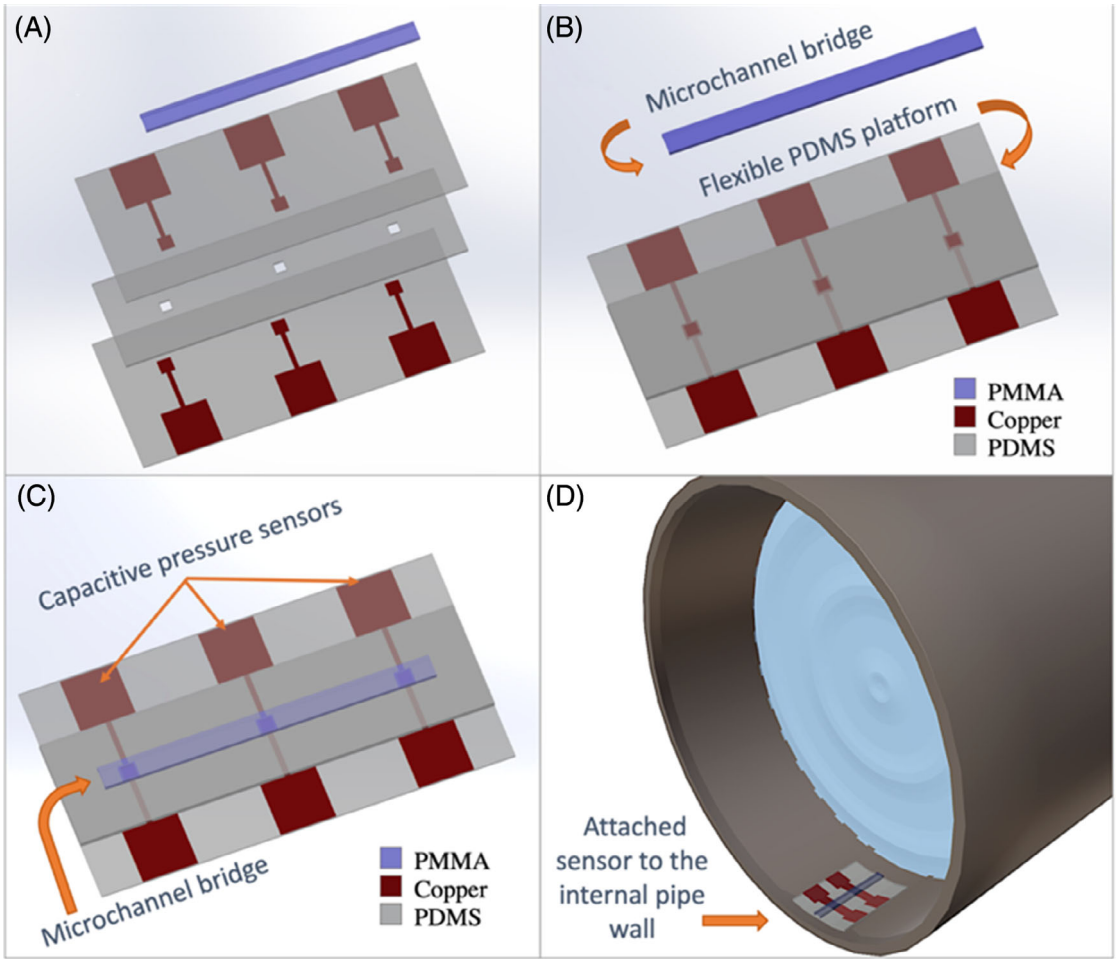

FIGURE 1 The materials used and structural design of the viscometer. (A) The sensor layers consist of three layers of PDMS and a microchannel bridge. (B) A physically flexible platform is developed with embedded capacitive pressure sensors. (C) The final form of the viscometer sensor with attached solid PMMA microchannel bridge to the physically flexible platform. (D) The sensor is anchored to the internal wall of a pipe to start monitoring the fluid viscosity in real-time

number. Equation (1) expresses the Reynolds number, where ρ is the fluid density, v is the average velocity, and μ is the dynamic viscosity.

$$Re = \frac{\rho v D_{\mathrm{h}}}{\mu} \tag{1}$$

The laminar flow is a mandatory condition for operating the viscometer that depends on the fluid velocity. Polydimethylsiloxane (PDMS) was chosen here as a flexible platform material because it provides a high flexibility and has earlier proven to be successful in microfluidic applications due to its excellent chemical and physical properties.[55] The PDMS platform uses the capacitive pressure sensors located below the microchannel as microfluidic flowmeters for the channel. The high flexibility of PDMS allows the platform to adopt different diameters of tubes and curved architectures when it is attached to the inner tube wall for viscosity measurements without the need for adjusting or re-calibrating the device. The sensor design has a moving-free structure built with long-lasting and low-cost materials including PMMA, PDMS, and copper for ensuring the device durability and affordability.

3 | OPERATING PRINCIPLE

The operating principle of the proposed viscosity sensor depends on the monitoring of the variation in flow rate according to the change in the fluid viscosity. Particularly, the fluid viscosity (μ) in the tubular system is inversely proportional to the

microfluid flow rate (Q) in the microchannel. Equation (2) expresses the relationship between the viscosity and flow rate using the Hagen-Poiseuille law for laminar flow. The equation is defined for channels with a rectangular cross-section, where w is the channel width, h is the channel depth, and ΔP is the pressure difference between two points separated by a distance L.

$$Q = \frac{\Delta P\, w^2\, h^3}{12\, \mu\, L\, (w + h)} \tag{2}$$

The fluid flow rate is the main detecting method for the fluid viscosity of the proposed sensor. At a constant flow rate of the pipe system, viscous fluids have lower flow rates inside the microfluidic channel than thin liquids, where it requires a higher pushing force or larger pressure difference to drag the liquid inside the microchannel. The change in the microfluidic flow rate is measured by the capacitive pressure sensors in the microchannel, where the total pressure (P_{Total}) comprises the dynamic (P_{Dynamic}) and the static (P_{Static}) pressures, as shown in Equation (3). The dynamic pressure is proportional to the square of the flow rate, as shown in Equation (4). In contrast, the static pressure depends on the fluid depth and density; thus, it has a smaller value as only a micro-depth of the channel is utilized. In Equation (4), ρ is the fluid density, h is the channel depth, g is the gravity acceleration, and A is the cross-sectional area of the channel. The measured capacitance and the absolute pressure are proportionally related as recognized from the capacitive pressure sensors.[56] Therefore, a change in the fluid viscosity is inversely proportional to the capacitance measurements due to the variation in the fluid flow rate.

$$P_{\text{Total}} = P_{\text{Static}} + P_{\text{Dynamic}} \tag{3}$$

$$P_{\text{Total}} = \rho\, h\, g + \frac{1}{2}\rho\frac{Q^2}{A^2} \tag{4}$$

4 | NUMERICAL SIMULATION

The operating principle and the effect of the microchannel depth were studied for the designed viscometer using a numerical simulation performed on a commercially available tool COMSOL. The analytical simulation was performed to understand the importance of the microchannel, to consider the effect of its depth on the device performance, to ensure fully developed flow conditions inside the microchannel, and, most importantly to understand the relationship between the fluid viscosity in the tubular system and flow rate in the microchannel. In the analysis, the fluid flow dynamics inside the 3-dimensional (3D) sensor system was replicated based on the Navier-Stokes equation of laminar flow.

We analyzed the pressure behavior in case of tubes 30 cm long but having different diameters and for a variety of fluid viscosities at a fixed flow rate equal to 2000 mL/min in the absence of a microchannel. The pressure measurements were recorded at a fixed individual point located at the base and in the middle of the tube length. Figure 2A shows the variation of the pipe diameter with different viscosity ranges and its effect on the pressure at the selected position. Each tube diameter has a different trend of performance with viscosity and diverse pressure ranges because the static pressure increases with pipe depth. Therefore, using a microchannel in a tube provides a uniform pressure range and behavior with viscosities depending on the microchannel flow rate and its constant depth.

In contrast, Figure 2B demonstrates the effect of the microchannel depth on the viscosity sensor performance at a measured point located at the center of the microchannel base. In the simulation, the microchannel was connected to the internal wall of a 4 cm diameter pipe with a fixed flow rate inside the pipe. The results show a consistent viscometer sensor performance for different microchannel depths with a dramatic decrease in the measured pressure when fluids with different viscosities are used. At higher fluid viscosities, the driven fluid in the microchannel as well as the absolute pressure decreases with dynamic pressure dominating the static pressure. At high viscosities, the flow rate and the dynamic pressure become too low, which allows the static pressure to develop particularly for the deeper channels, as shown for the 450 μm depth. Figure 3 proves the previous interpretation to be true by describing the absolute pressure at the same conditions using a 250 μm deep channel. The total pressure is almost equal to the dynamic pressure; hence, the static measurements are negligible compared to the dynamic measurements. Moreover, the dynamic pressure behavior follows the trend of the microchannel flowrate as expected.

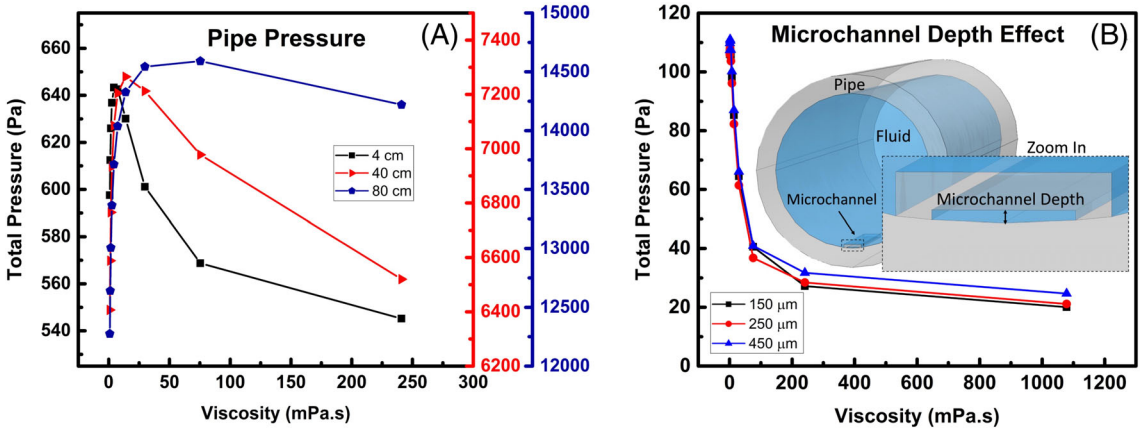

FIGURE 2 Study the depth effect on the viscometer performance. (A) Without using a microchannel, the pressure behavior and its range are highly influenced by tube depths. (B) The microchannel provides a uniform response and ensures smooth pressure transitions in the viscosity sensor

FIGURE 3 Analyze the pressure components at a point centered on the base of a 250 μm channel depth attached to the 4 cm diameter pipe. The pipe has a steady flow rate equivalent to 2000 mL/min, and the microchannel has a fluid viscosity-dependent flow rate

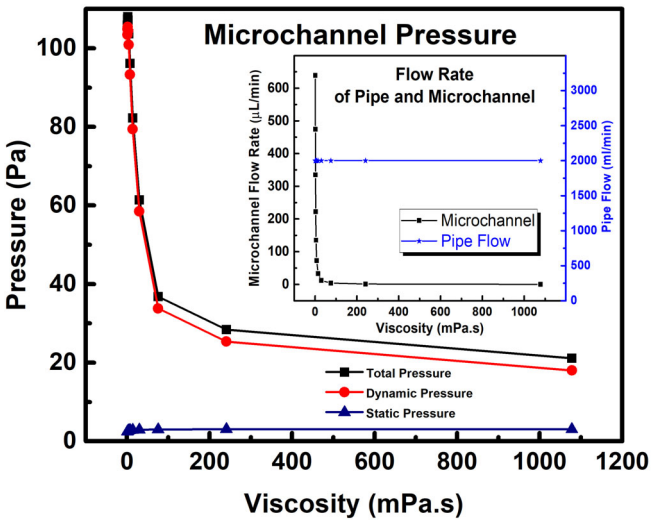

5 | FABRICATION PROCESS

The viscometer was fabricated using a lithography-free process to make it inexpensive. The flow sensor consists of two main parts: the PMMA microchannel bridge and the mechanically flexible PDMS platform installed with embedded capacitive pressure sensors. The flexible platform was fabricated utilizing three treated PDMS layers; each layer is 500 μm thick. The first and last layers were sputtered with 200 nm of copper to form the lower and upper conductive plates of the capacitance sensors, respectively. Kapton tape patterned with a CO_2 laser to create 3 mm wide squares was used as a shadow mask as the capacitance active area. The PDMS surface was treated with oxygen plasma to convert the hydrophobic surface to hydrophilic by increasing the surface roughness and improving the metal adhesion on the surface before sputtering with copper. The second and the middle layer was patterned with the CO_2 laser crossing through the entire depth of the PDMS layer to form 3 mm wide square trenches as a cavity for the dielectric of the capacitance sensors. Then, the three developed PDMS layers were arranged in order and combined to form the platform by the oxygen plasma bonding technique. The surfaces of the layers were exposed to oxygen plasma for 60 seconds, followed by direct contact between the surfaces, and subsequently 60 seconds of platform baking at 80°C as a bond enhancement procedure. The copper electrodes were bonded to flexible wires using a silver paste. After that, the platform was packed with a PDMS layer to protect the connections and the copper electrodes as well as to affix the positions of the layers and prevent air leaking. Figure 4A illustrates the final form of the fabricated PDMS platform with the embedded capacitive sensors.

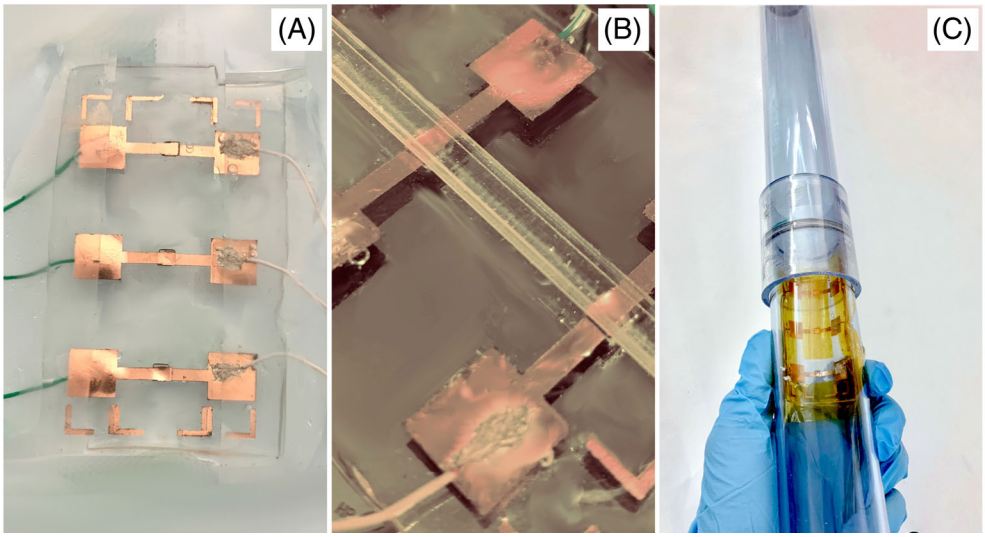

FIGURE 4 The fabrication process for the viscometer. (A) The mechanically flexible PDMS platform with the embedded capacitive sensors. (B) Attaching the PMMA microchannel bridge on the PDMS platform. (C) Attached the viscometer to the internal PVC pipe walls

The microchannel bridge was fabricated using a 1 mm thick PMMA sheet, which was patterned using the CO_2 laser to form a microchannel bridge with a 3 mm wide and 60 mm long rectangular trench having a 250 μm depth. Then, the microchannel bridge was attached to the prepared flexible platform using the oxygen plasma bonding technique, as shown in Figure 4B. The device was repackaged with a thin PDMS coat to ensure proper bonding and secure the microchannel position on the platform while preventing the clogging of the channel inlet and outlet.

A laboratory pipe setup was constructed using a transparent polyvinyl chloride (PVC) pipe having a 3.8 cm inner diameter and a 60 cm total length of the system. The pipe system was well encapsulated with caps and fastened with epoxy glue. The pipe inlet and outlet were connected to the pump tubing having a 6.4 mm internal diameter. The viscometer was installed on the interior wall of the tube using Kapton tape with Silicone adhesive before building the setup. The sensor was placed at a distance of 15 cm as the calculated hydrodynamic entrance depends on the length-to-step height ratio of the inlet of the liquid. Figure 4C shows the viscometer attached to the internal walls of the PVC pipe system. A pipe having a 4 cm outer diameter was selected for the laboratory characterization suitable for small pipe diameters for demonstrating the mechanical flexibility of the device and using it to minimize the fluid volume for the testing samples. However, it is also compatible with larger pipe diameters as the mechanically flexible platform flattens when a larger bending radius is used.

5.1 | Characterization and results

Figure 5 displays the characterization setup for the real-time monitoring of fluid viscosity in the pipe system. A pump controller (Catalyst FH100DX Pump) was used to drive the fluid from the fluid reservoir to the pipe system at a steady flow of 2000 mL/min. The sensor was tested with diverse fluid viscosities. Volume-diluted glycerol solutions and lubricant oils with international standards organization viscosity grade (ISO VG) were used to characterize the sensor at different viscosities with pre-known values. Two liters of the liquid samples were used for each viscosity test, which could fill the pipe and pumping tubes and leave some liquid in the reservoir for pumping. Each fluid's characterization was done separately to prevent liquid waste by filling the pipe with a fluid sample to run the test. The pipe system was then drained from the liquid, refilled with a new fluid sample, and stored the previously used fluid for later usage. The capacitance was measured with Keithley for each running fluid, and a switch was used to allow altering between different capacitor sensors. The $\Delta C/Co$ value was calculated for the measured capacitance to investigate the change in capacitance in response to the difference in the microfluidic flow rate due to the change in the fluid viscosity. Here, C and Co are the capacitance values with and without the applied pressure, respectively.

Figure 6 presents the viscometer characterization results for a capacitor sensor located at the center of the microchannel base. A resolution higher than 2.7 mPa s for a wide of viscosity range from 4 to 334 mPa s is seen. The results for the diluted glycerol solutions and the lubricant oils show similar and repeatable behaviors. The capacitance pressure sensor represents the microchannel flow rate that is inversely related to the fluid viscosity, as the numerical simulation claims.

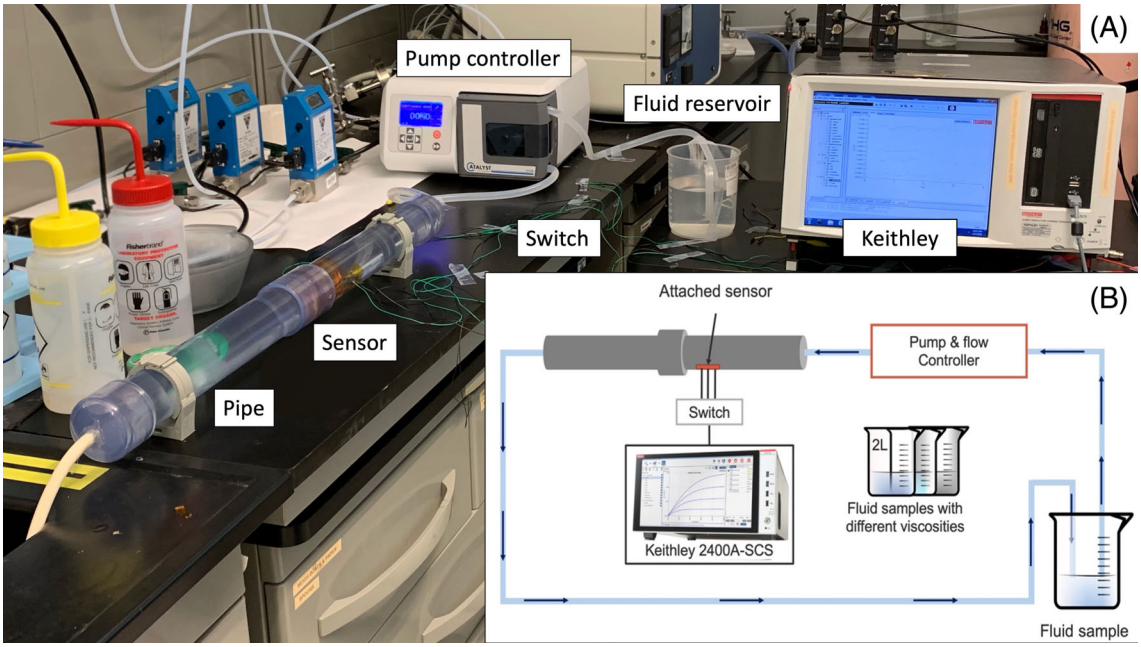

FIGURE 5 Viscometer characterization setup for real-time monitoring of fluid in a pipe system

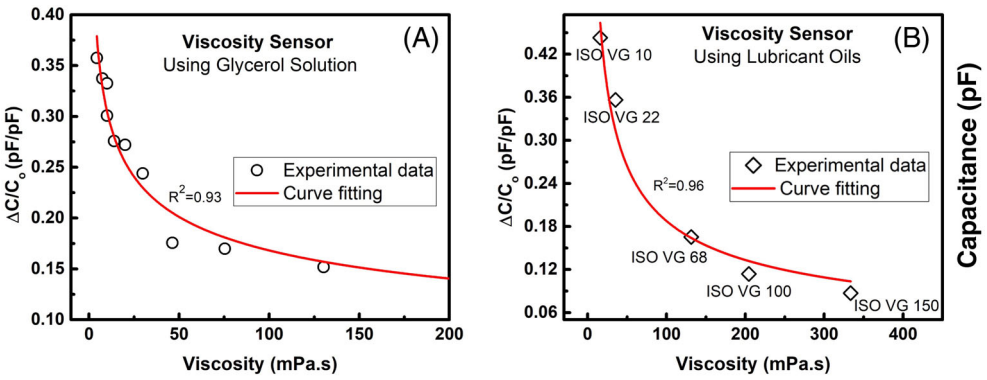

FIGURE 6 Viscometer characterization results (A) using several diluted glycerol solutions (B) using different ISO VG lubricant oils

The change in the capacitance value is interpreted to the dynamic viscosity as expressed in Equation (5). It is based on the power fitting curve function of the plotted data, where C is the capacitance value in pF, and μ is the dynamic viscosity in mPa s.

$$C = 6.828 \frac{1}{\mu^{0.099}} \tag{5}$$

Highly viscous fluids exhibit lower forces to drive the fluids into the microchannel at a steady pipe flow, thereby causing a decrease in the microfluidic flowrate that is translated into a reduction in the capacitive measurements. The results show a sensitivity of upto 4.18 pF/pF, which is equivalent to 88 Pa for each 1 Pa s change in the fluid viscosity ranging from 0 to 50 mPa s. The calibration method of the capacitive sensor with pressure is shown in Supplementary Figure 1. The capacitive pressure sensors were characterized using Keithley at different water depths.

The sensor was further integrated with commercially purchased electronic devices to create a standalone functional system installed inside the pipe, as illustrated in Figure 7A,B. Bluetooth low energy (BLE) enabled programmable system on chip (PSoC) was chosen as the central electronic interface procured from Cypress. It contains an internal capacitance to digital convertor (CDC) to connect the three capacitive sensors to the electronic interface without the need for additional integrated circuits (ICs) or passive components, as shown in the Supplementary Figure 2a. The raw CDC values

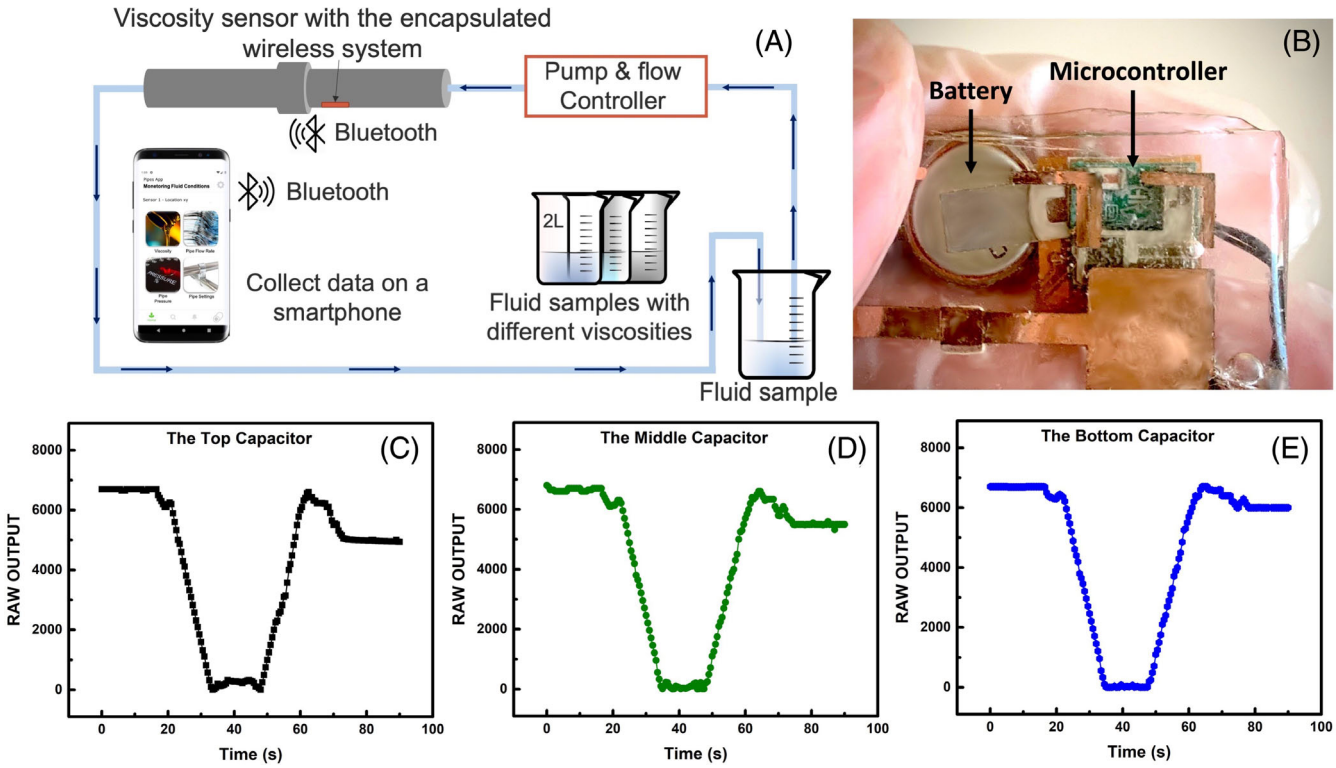

FIGURE 7 Stand-alone system for real-time measurements using a wireless data transfer. (A) Illustration of the system application for continuous tracking of the viscosities transformation of the fluids. (B) The electronic interface includes a BLE that enabled the PSoC chip and a coin battery power supply. (C) The output response against time for the pressure sensor at the top, (D) middle, and (E) bottom. The *y*-axis shows the output response from BLE PSoC in a raw capacitive to digital convertor values

can be converted into a capacitance unit using the calibration plot shown in the Supplementary Figure 2b. The calibration graph was generated using different commercial capacitors and measured using the chip. Furthermore, the PSoC has the built-in BLE functionality to enable wireless data transmission through the pipe. The system was powered using a coin cell battery due to the advantage of the low power consumption of the chip. The complete electronic interface was connected to the sensors and packaged via PDMS for insulation. For the plastic pipe having 4 cm diameter and filled with fluid, the BLE can easily communicate with any device in a 10 m range, where a 50 m field is unobstructed. A test was performed with the sensor connected to the electronic interface, and the sensor was submerged in water upto depth of 50 cm (Supplementary Video 1). The real-time data measured by the three sensors were sent to the smartphone shown in the video. The plots of the experimental data obtained from the three sensors are shown in Figure 7C-E. However, an alternative wireless data transmission technology is needed for metal tube systems or pipes with diameters larger than the tested range.

6 | CONCLUSION

In summary, we have reported a new application method of a microfluidic viscometer that depends on the flow rate change to allow real-time monitoring of fluids in pipe systems. The novel design of the device ensures a negligible pressure drop or fluid disturbance compared to the bulky monitoring sensors due to the microchannel and the mechanically flexible platform adaptable for different pipe diameters and surfaces. The microchannel ensures a laminar flow in the sensing area regardless of the flow type in the pipe. Moreover, the bridge design for the microchannel ensures the fluid driving force from the pipe to the microchannel without the need for a pumping system or manually withdrawn samples. In addition, the sensor was fabricated using low-cost materials and lithography-free procedures for affordability. The numerical simulation shows the importance of using the microchannel for a predictable sensor behavior and provides a bounded pressure range, regardless of the tube diameter and without the need for re-calibrating or modifying the sensor.

The experimental results match those of the simulation analysis, where both show that at a constant pipe flow rate, the viscosity is inversely related to the measured pressure due to the change in the microfluidic flow rate. The sensor was capable of measuring different fluid viscosities over a wide range from 4 to 334 mPa s with a resolution higher than 2.7 mPa s. A stand-alone system was integrated with the sensor for real-time monitoring using wireless communication between the viscometer and smartphone for a plastic pipe system filled with liquids and having upto 50 cm pipe diameters.

ACKNOWLEDGEMENTS

This publication is based on the work supported by King Abdullah University of Science and Technology (KAUST) and the Research and Development Centre of Saudi Aramco company.

PEER REVIEW INFORMATION

Engineering Reports thanks Karla Mossi and other anonymous reviewers for their contribution to the peer review of this work.

PEER REVIEW

The peer review history for this article is available at https://publons.com/publon/10.1002/eng2.12315.

CONFLICT OF INTEREST

The authors declare no potential conflict of interest.

DATA AVAILABILITY STATEMENT

The data that support the findings of this study are available from the corresponding author upon reasonable request.

ORCID

Muhammad M. Hussain https://orcid.org/0000-0003-3279-0441

REFERENCES

1. Adegboye MA, Fung W, Karnik A. Recent advances in pipeline monitoring and oil leakage detection technologies: principles and approaches. *Sensors*. 2019;19:2548.
2. Piroozian A, Ismail I, Yaacob Z, Babakhani P, Ismail ASI. Impact of drilling fluid viscosity, velocity and hole inclination on cuttings transport in horizontal and highly deviated wells. *J Petrol Explor Prod Technol*. 2012;2:149-156.
3. Zhao Y, Yeung H, Zorgani EE, Archibong AE, Lao L. High viscosity effects on characteristics of oil and gas two-phase flow in horizontal pipes. *Chem Eng Sci*. 2013;95:343-352.
4. Muñoz JAD, Ancheyta J, Castañeda LC. Required viscosity values to ensure proper transportation of crude oil by pipeline. *Energy Fuel*. 2016;30:8850-8854.
5. Thorat S, Thibodeau C, Collier B, Ngo H. Leveraging control and monitoring technologies. *IEEE Indus Appl*. 2017;23:62-73.
6. Covitch MJ, Trickett KJ. How polymers behave as viscosity index improvers in lubricating oils. *Adv Chem Eng Sci*. 2015;5:134-151.
7. Mahmood W, Mohammed A, Ghafor K. Viscosity, yield stress and compressive strength of cement-based grout modified with polymers. *Results Mater*. 2019;4:100043.
8. Maazouz A, Lamnawar K, Dkier M. Chemorheological study and in-situ monitoring of PA6 anionic-ring polymerization for RTM processing control. *Compos Part A*. 2018;107:235-247.
9. Postnov DD, Moller F, Sosnovtseva O. Dairy products viscosity estimated by laser speckle correlation. *PLoS One*. 2018;13(1–10):e0203141.
10. Bista A, Hogan SA, O'Donnell CP, Tobin JT, O'Shea N. Evaluation and validation of an inline Coriolis flowmeter to measure dynamic viscosity during laboratory and pilot-scale food processing. *Innov Food Sci Emerg Technol*. 2019;54:211-218.
11. Yunoki S, Sugimoto K, Ohyabu Y, Ida H, Hiraoka Y. Accurate and precise viscosity measurements of gelatin solutions using a rotational rheometer. *Food Sci Technol Res*. 2019;25:217-226.
12. Zangabad R, Bahrami M. Capillary-type mass flow meter. *Measurement, Instrumentation, and Sensors Handbook*. Boca Raton: CRC Press; 2014:1-13. https://doi.org/10.1201/b15474-57.
13. Oh S, Kim B, Lee JK, Choi S. 3D-printed capillary circuits for rapid, low-cost, portable analysis of blood viscosity. *Sens Actuat B*. 2018;259:106-113.
14. Yulkifli Y, Kurniati R. Development of digital viscometer based on sensor technology and microcontroller. *J Phys Conf Ser*. 2018;1040:1–8.
15. Lu X, Hou L, Zhang L, Tong Y, Zhao G, Cheng ZY. Piezoelectric-excited membrane for liquids viscosity and mass density measurement. *Sens Actuat A Phys*. 2017;261:196-201.
16. Clara S, Feichtinger F, Voglhuber-Brunnmaier T, Niedermayer AO, Tröls A, Jakoby B. Balanced torsionally oscillating pipe used as a viscosity sensor. *Meas Sci Technol*. 2019;30:015101.
17. Junker C, Meier K. Analysis of the electrical field in viscosity sensors with torsionally vibrating quartz cylinders. *J Appl Phys*. 2020;128:044505.

18. Gonzalez M, Seren H, Buzi E, Deffenbaugh M. Fast downhole fluid viscosity and density measurements using a self-oscillating tuning fork device. *2017 IEEE Sensors Applications Symposium (SAS)*. Glassboro: IEEE; 2017:1-5. https://doi.org/10.1109/SAS.2017.7894045.
19. Yunus M, Arifin A. Design of oil viscosity sensor based on plastic optical fiber. *Journal of Physics: Conference Series*. 2018;979:012083. http://dx.doi.org/10.1088/1742-6596/979/1/012083.
20. Lee S-C, Heo J, Woo HC, et al. Fluorescent molecular rotors for viscosity sensors. *Chem A Eur J*. 2018;24:13706-13718.
21. Camas-Anzueto JL, Gómez-Pérez J, Meza-Gordillo R, et al. Measurement of the viscosity of biodiesel by using an optical viscometer. *Flow Meas Instrum*. 2017;54:82-87.
22. Jiang T, Li J, Zhang S. Design of a new structure for rotary viscometer. *Materials Science and Engineering*. Vol 782. Qingdao: IOP Publishing; 2020.
23. Fabritius T, Kinnunen P and Czajkowski J. Dual measurement mode rotational viscometer. *2020 IEEE International Instrumentation and Measurement Technology Conference (I2MTC)*. Dubrovnik, Croatia: IEEE; 2020;1-5. https://doi.org/10.1109/I2MTC43012.2020.9129561. Accessed May 27, 2020.
24. Kim YJ, Cho B, Lee S, Hu J, Wilde JW. Investigation of rheological properties of blended cement pastes using rotational viscometer and dynamic shear rheometer. *Adv Mater Sci Eng*. 2018;2018:6.
25. Durdag K, Andle J. Real-time viscosity measurement for condition-based monitoring using solid-state viscosity sensor. *Tribol Trans*. 2008;51:296-302.
26. Nour MA, Hussain MM. A review of the real-time monitoring of fluid-properties in tubular architectures for industrial applications. *Sensors*. 2020;20(14):1–22.
27. Berta M, Wiklund J, Kotzé R, Stading M. Correlation between in-line measurements of tomato ketchup shear viscosity and extensional viscosity. *J Food Eng*. 2016;173:8-14.
28. Meacci V, Ricci S, Wiklund J. Flow-Viz – an integrated digital in-line fluid characterization system for industrial applications. *IEEE Sens*. 2016;2:1-6.
29. Raffer, G. *Rotational Viscometer*. US009261446B2. 2016.
30. Hosoda M, Yamakawa Y, Sakai K. Continuous in-line measurement of viscosity using self-balancing electro-magnetically spinning technique. *Jpn J Appl Phys*. 2020;59:SKKA09.
31. Carapelli G. Viscosity dependent flow meter for use in fuel dispensing environments, US9377332B2. 2014.
32. Wiklund J, Stading M, Trägårdh C. Monitoring liquid displacement of model and industrial fluids in pipes by in-line ultrasonic rheometry. *J Food Eng*. 2010;99:330-337.
33. Gul S, Erge O, van Oort E. Frictional pressure losses of non-Newtonian fluids in helical pipes: applications for automated rheology measurements. *J Nat Gas Sci Eng*. 2020;73:103042.
34. Biswas S, Winoto SH. Prediction of pressure drop in non-woven filter media using a Hagen-poiseuille model. *Tribol Trans*. 2000;43:251-256.
35. Eu BC. Generalization of the Hagen–Poiseuille velocity profile to non-Newtonian fluids and measurement of their viscosity. *Am J Phys*. 1990;58:83-84.
36. Wiklund J, Haldenwang R. Application of ultrasound Doppler technique for in-line rheological characterization and flow visualization of concentrated suspensions. *Can J Chem Eng*. 2016;94:1066-1075.
37. Gottlieb, E. J. *Ultrasonic Viscometer*. US20160187172A1. 2016.
38. Shih JL, Kobayashi M, Jen CK. Flexible metallic ultrasonic transducers for structural health monitoring of pipes at high temperatures. *IEEE Trans Ultrason Ferroelectr Freq Control*. 2010;57:2103-2110.
39. Mortensen NA, Bruus H. Universal dynamics in the onset of a Hagen-Poiseuille flow. *Phys Rev E*. 2006;74:017301.
40. O'Shea N, O'Callaghan TF, Tobin JT. The application of process analytical technologies (PAT) to the dairy industry for real time product characterization - process viscometry. *Innov Food Sci Emerg Technol*. 2019;55:48-56.
41. Pfusterschmied G, et al. Sensing fluid properties of super high viscous liquids using non-conventional vibration modes in piezoelectrically excited mems resonators. Paper presented at: 2019 IEEE 32nd International Conference on Micro Electro Mechanical Systems (MEMS); 2019: IEEE:735–738.
42. Maurya RK, Kaur R, Kumar R, Agarwal A. A novel electronic micro-viscometer. *Microsyst Technol*. 2019;25:3933-3941.
43. Choudhary S. *Improvements to a Thermally Actuated MEMS Viscosity Sensor*. New York, NY: Rochester Institute of Dent Tech; 2019.
44. Yu S, Wang S, Lu M, Zuo L. Review of MEMS differential scanning calorimetry for biomolecular study. *Front Mech Eng*. 2017;12:526-538.
45. Jiang C, Chen Y, Cho C. A three-dimensional finite element analysis model for SH-SAW torque sensors. *Sensors*. 2019;19:4290.
46. Kolliopoulos P, Jochem KS, Lade RK, Francis LF, Kumar S. Capillary flow with evaporation in open rectangular microchannels. *Langmuir*. 2019;35:8131-8143.
47. Feng D, Li X, Wang X, Li J, Zhang X. Capillary filling under nanoconfinement: the relationship between effective viscosity and water-wall interactions. *Int J Heat Mass Trans*. 2018;118:900-910.
48. Whitesides GM. The origins and the future of microfluidics. *Nature*. 2006;442:368-373.
49. Bamshad A, Nikfarjam A, Sabour MH. Capillary-based micro-optofluidic. *Meas Sci Technol*. 2018;29:13.
50. Solomon DE, Abdel-Raziq A, Vanapalli SA. A stress-controlled microfluidic shear viscometer based on smartphone imaging. *Rheologica Acta*. 2016;55:727-738.
51. Kohl MJ, Abdel-Khalik SI, Jeter SM, Sadowski DL. A microfluidic experimental platform with internal pressure measurements. *Sens Actuat A Phys*. 2005;118:212-221.
52. Elbuken C, Glawdel T, Chan D, Ren CL. Detection of microdroplet size and speed using capacitive sensors. *Sens Actuat A Phys*. 2011;171:55-62.

53. Majarikar V, Takehara H, Ichiki T. Microcapillary electrophoresis chip with a bypass channel for autonomous compensation of hydrostatic pressure flow. *Microfluidics Nanofluidics*. 2018;22(10):1–7.
54. Viscometer/rheometer-on-a-Chip. VROC Technology. *rheosense*. https://www.rheosense.com/technology.
55. Mata A, Fleischman AJ, Roy S. Characterization of polydimethylsiloxane (PDMS) properties for biomedical micro/nanosystems. *Biomed Microdevices*. 2005;7:281-293.
56. Puers R. Capacitive sensors: when and how to use them. *Sens Actuat A Phys*. 1993;38:93-105.

SUPPORTING INFORMATION

Additional supporting information may be found online in the Supporting Information section at the end of this article.

How to cite this article: Nour MA, Khan SM, Qaiser N, Bunaiyan SA, Hussain MM. Mechanically flexible viscosity sensor for real-time monitoring of tubular architectures for industrial applications. *Engineering Reports*. 2020;e12315. https://doi.org/10.1002/eng2.12315